
AnyLogo: Symbiotic Subject-Driven Diffusion System with Gemini Status

Jinghao Zhang^{1*} Wen Qian² Hao Luo^{2,3} Fan Wang² Feng Zhao^{1†}

¹University of Science and Technology of China,

²DAMO Academy, Alibaba Group ³Hupan Lab, Zhejiang Province

Abstract

Diffusion models have made compelling progress on facilitating high-throughput daily production. Nevertheless, the appealing customized requirements are remain suffered from instance-level finetuning for authentic fidelity. Prior zero-shot customization works achieve the semantic consistence through the condensed injection of identity features, while addressing detailed low-level signatures through complex model configurations and subject-specific fabrications, which significantly break the statistical coherence within the overall system and limit the applicability across various scenarios. To facilitate the generic signature concentration with rectified efficiency, we present **AnyLogo**, a zero-shot region customizer with remarkable detail consistency, building upon the symbiotic diffusion system with eliminated cumbersome designs. Streamlined as vanilla image generation, we discern that the rigorous signature extraction and creative content generation are promisingly compatible and can be systematically recycled within a single denoising model. In place of the external configurations, the gemini status of the denoising model promote the reinforced subject transmission efficiency and disentangled semantic-signature space with continuous signature decoration. Moreover, the sparse recycling paradigm is adopted to prevent the duplicated risk with compressed transmission quota for diversified signature stimulation. Extensive experiments on constructed logo-level benchmarks demonstrate the effectiveness and practicability of our methods.

1 Introduction

Diffusion models have demonstrated impressive capabilities in creative content generation, such as marvelous image generation [1, 2, 3, 4], image manipulation [5, 6, 7, 8], video generation [9, 10, 11, 12], audio synchronized [13, 14, 15, 16], *etc.*, and profoundly impact the practice of the public daily production. Large volume of the generative requests necessitate the expeditious response, while the appealing customized aspirations are remain suffered from instance-level finetuning for authentic fidelity. Prosperously, recent efforts have been witnessed toward the zero-shot customization with single forward pass, which achieve the semantic consistency through the condensed injection of identity features, applications involving the object-level manipulation [17, 18, 19, 20], facial fidelity generation [21, 22, 23, 24], *etc.* while the meticulous low-level signatures are less concentrated.

In this regard, we may entertain that *are we really need the low-level signatures in daily customization*. Beyond the semantic recognizable similarities, there are numerous fidelity-disciplined sceneries such as text glyph generation [25, 26, 27], image character animation [28, 29, 30, 31], virtual tryon [32, 33, 34], *etc.*, that strive for the extraordinary signature consistency with lower vision tolerance. Moreover, the brand logo customization drastically involves the copyright license, which overwhelming the moderate semantic injection insufficient for the signature-consistent customization,

*This work was done during an internship at Alibaba Group. This work was supported by Alibaba Group through Alibaba Research Intern Program.

†Corresponding author.

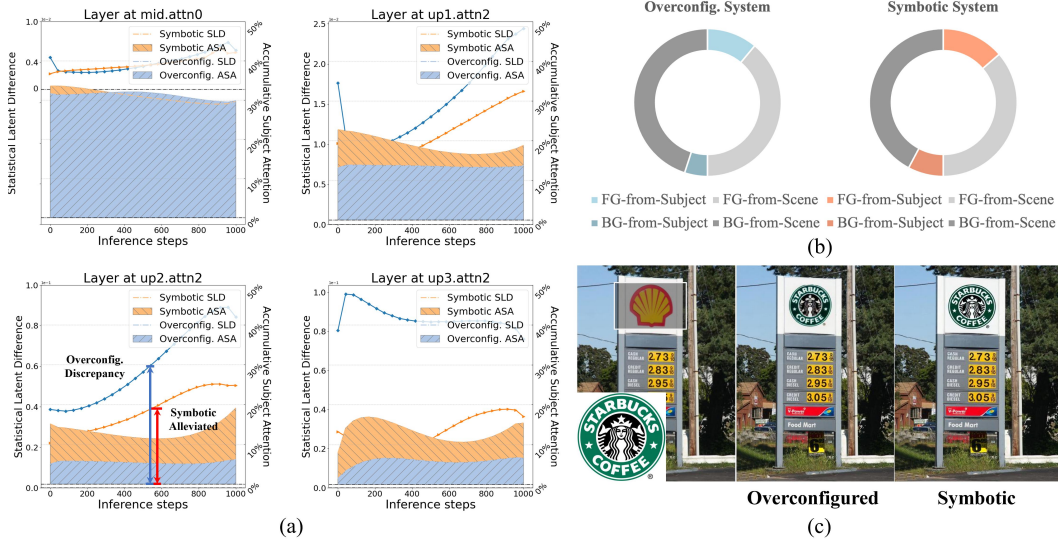


Figure 1: The comparison of the **overconfigured system** and the **symbiotic system** in transmission efficiency. (a) The proportion of the accumulative subject attention (ASA) and the transmitted statistic latent difference (SLD) at four distributed self-attention layers in the denoising model, where the SLD is computed between the transmitted subject latents and the corresponding denoising latents. The symbiotic system raises the increasing transmission efficiency with deeper model operations. (b) The comprehensive attention analysis accumulated along the model layers and the denoising steps. Both the customized region (light) and the background area (dark) benefit the boosted subject expertise from the symbiotic system. (c) Visual comparison results of two subject-driven diffusion systems. Detailed calculation process and visual illustration of two systems are provided in Appendix E.

as shown in Fig. 5. Current practices incorporate the auxiliary configured ControlNet [25, 33, 35] and ReferenceNet [29, 30, 36] for reinforced detail enhancement through progressive residual complement or hierarchical mutual spatial attention. However, the complex model overconfigurations significantly break the statistical coherence within the overall system, as shown in Fig. 1 (a), resulting in suboptimal signature transmission efficiency with declined proportion of the accumulated subject attention score, which we referred as *overconfigured system*. Besides, there are also specialized attempts involving the utilization of the OCR model in precise text generation [25] and the posture steered warping operation in tryon application [33, 34], however, the subject-specific fabrications considerably narrow the applicable scenario potential. In light of this, it is prospective to facilitate the generic signature concentration in daily customization with rectified transmission efficiency.

To this end, we present AnyLogo, a zero-shot region customizer with remarkable low-level signatures consistency, proficient in diversified graphic patterns and text glyphs. Streamlined as vanilla image generation, AnyLogo is built upon the symbiotic diffusion system with economic model recycling policy, where we discern that **the rigorous signature extraction and creative content generation can be systematically recycled within a single denoising network**. The symbiotic diffusion system manifest the promisingly compatible generation capability with several peculiarities:

- In place of the external configuration, the gemini status of the denoising network, *i.e.*, the signature extraction and content generation largely alleviate the statistic coherence of the system owing to the self-delivery, yielding efficient signature transmission with reinforced subject attention, as shown in Fig. 1 (a) and (b). And the efficiency raised by symbiotic system manifests the increased momentum as more operations within the denoising model.
- The low-level signatures derived from the symbiotic system is highly semantic-independent, where the native diversified generation capability is conserved with blocked signature delivering, which is disparate from the collapsed status in overconfigured systems, as shown in Fig 4. Moreover, the symbiotic system enjoy the continuous signature decoration space.

Apart from that, the overloaded signatures generically incur the potential duplicated risk. Preceding works introduce various compressed signals such as landmark representation [36], high-frequency map [33, 35] for signature delivering, which is unaccommodated to the symbiotic system owing to

the altered signal states. In consequence, we adopt the sparse recycling paradigm with randomly discarding the self-delivered signatures for trimmed transmission quota, stimulating diversified hyper-representations of the signature with scene harmonization. Additionally, we show that Anylogo also supports the diversified highlight of the specified subject area with sensible background translation.

To comprehensively evaluate our method, a logo-level customization benchmark is constructed, involving $\sim 1k$ high-quality pairs with rich textures, collecting from the open source wild logo detection datasets, tryon datasets with brand annotation, and text glyph datasets. Extensive experiments on constructed benchmarks demonstrate the effectiveness and practicability of our methods.

2 Related work

2.1 Prompt-driven Image Region Manipulation

Creative and convenient image region manipulation has attracted increasing number of people to exercise in their daily production, accredited to the remarkable progress of the prevailing generative model. Basically, the user practice can be categorized into the following three paradigms. The text-driven image region manipulation [37, 38, 39, 40] operates the candidate region with single text prompt, which specifies the desired attribute or object in principle, result in semantic aligned appearance. Despite the flexibility, the precise control manifests to be imperative. The image-driven image region manipulation [17, 18] transports the image prompt to the candidate region, delivering the concrete manipulative intention, result in content preservation and realistic outlook. Traditional image composition methods have investigated such aspiration for a long while, including image harmonization [41, 42], image blending [43, 44], and geometric correction [45, 46]. However, the intricate subbranches perplex the feasible pipelines, and the low-level manipulation is more concentrated with restricted semantic conformity. Recent diffusion models [1, 2] have shown impressive image composition capability, which incorporate the image prompt into the denoising process through condensed encoding embedding injection [17, 18, 20, 47]. While the details are further complemented with low-level feature interaction [35, 48, 49, 50]. Toward the synergic, the multimodal-driven image manipulation [51, 8] are further investigated with interleaved text and image prompt, fortified with multimodal large-language models for diversified token injection.

2.2 ID-preserved Image Generation

ID-preserved image generation is widely requisite in applications. Prior works on customized concept learning [52, 53, 54, 55, 56] generate subject-relevant images with arbitrary text prompt in few of user provided images. However, the optimization typically involves the intensive instant-level finetuning, which is cumbersome for large-scale deploy. To this end, recent efforts on facial identity preservation [36, 21, 22, 23, 24] accomplish the customization with a single forward pass, depending on the injection of the identity feature extracted from CLIP or facial model, result in the semantic recognizable fidelity and flexible text controllability. In the field of human animation, the image-to-video methods [30, 28, 29, 12, 57] generate the reference-based video sequences following the motion signals, and relies heavily on the identity consistency. The common practice predefine the configured ControlNet or ReferenceNet to retain precious subject details with hierarchical representation interaction, result in impressive id preservation. Additionally, there are also attempts toward the training-free customization [48, 49, 58, 59] through multi-branch attention manipulation with paralld reconstructive diffusion processes, albeit the flexibility, they reckon on the pretrained model with confined fidelity and concentrate on the original text-driven manipulation.

3 Method

In this section, we provide a brief background of the text-to-image diffusion models and current subject-driven customization practices in Sec. 3.1. Then, we introduce our symbiotic diffusion system built with model recycling policy in Sec. 3.2. The sparse recycling with compressed transmission quota is presented in Sec. 3.3. Finally, we briefly show the data collection criterion in Sec. 3.4.

3.1 Preliminary

Diffusion models [60, 61, 62, 63] were introduced as latent variable generative models with forward and reverse Markov chain, which gradually perturb the data with noise until tractable distribution and reverse the process with score matching or noise prediction for sampling. Combined with prompt conditions, diffusion models are capable of generating images with aligned user aspiration. In this work, we conduct experiments on the prevailing Stable Diffusion [1], which comprises an encoder $\mathcal{E} : \mathcal{X} \rightarrow \mathcal{Z}$, and a decoder $\mathcal{D} : \mathcal{Z} \rightarrow \mathcal{X}$, where $\hat{x} = \mathcal{D}(\mathcal{E}(x))$. The denoising network ϵ_θ is operated in the latent space with attached conditional encoder τ_θ . The training objective for stable diffusion is to minimize the denoising objective by

$$\mathcal{L} = \mathbb{E}_{z,c,\epsilon,t} [\|\epsilon - \epsilon_\theta(z_t, t, \tau_\theta(c))\|_2^2], \quad (1)$$

where z_t is the latent feature at timestep t , and c is the given prompt condition.

Precedent customization methods involving instance-level optimization on specific subject with prior preservation loss [52, 56] or concept embedding [53, 54]. Recent practices on zero-shot customization largely derive from the stable diffusion and substitute the conditional encoder τ_θ with image modal for semantic injection. Moreover, the low-level signatures are complemented with paralleled model configurations such as ControlNet or ReferenceNet, which formulate the denoising network as $\epsilon_\theta(z_t, t, \tau_\theta(c), \zeta_\theta(\mathcal{T}(c)))$, where ζ_θ provides the hierarchical subject interactions, and \mathcal{T} is the transformation for delivering diversified hint signals [35] with potential information bottleneck.



Figure 2: Preliminary of the informative latents in diffusion model. (a) Exclude the impact from the public VAE component, where the zoom-in reconstruction show almost spotless fidelity. (b) Without bells and whistles, the inversion technique reproduce the original image with single initial noise, the negligible deviation implying the great signature potential within the denoising model.

3.2 Symbiotic Diffusion System with Model Recycling

The intermediate latents in diffusion models contain rich semantic clues and copious fine-grained details [64, 65, 66], while the derived downstream applications range from zero-shot classification, segmentation, to generative prompt-driven manipulation [67, 68], and 3D rendering [69, 70]. As shown in Fig. 2 (a), we first exclude the impact from the public VAE component, where the decoded vae latents with zoom-in transmission disclose the almost spotless fidelity, *i.e.*, $\hat{x} \simeq x$, implying the disengagement of the signature conservation. Additionally, without bells and whistles, the glamorous images can be exactly generated through advanced diffusion inversion techniques [71] with single initial noise, *i.e.*, $x \simeq \mathcal{D}(\Gamma(z_t, t, \epsilon_\theta(z_t, t, \tau_\theta(c))))$, where Γ is the noising schedule updated from $t : T \rightarrow 0$, and $z_T = \Gamma^{-1}(z_t, t, \epsilon_\theta(z_t, t, \tau_\theta(c)))$ obtained from $t : 0 \rightarrow T$. As shown in Fig. 2 (b), the appealing fidelity indicates the huge potential of the latent denoising model in signature collection, transmission, and representation along the denoising process. Therefore, we suppose that *the denoising network ϵ_θ is sufficient for grasping the informative evidence we would desired about the signature*. Disparate from prevailing approaches that dedicated to the external overconfigured assistant models ζ_θ , we made efforts toward the inside diffusion system for holistic efficiency.

Task Formulation. We consider the subject-driven region customization, which ordinarily necessitate the scrupulous signature-level consistency, compared to the full-size image generation. The overall

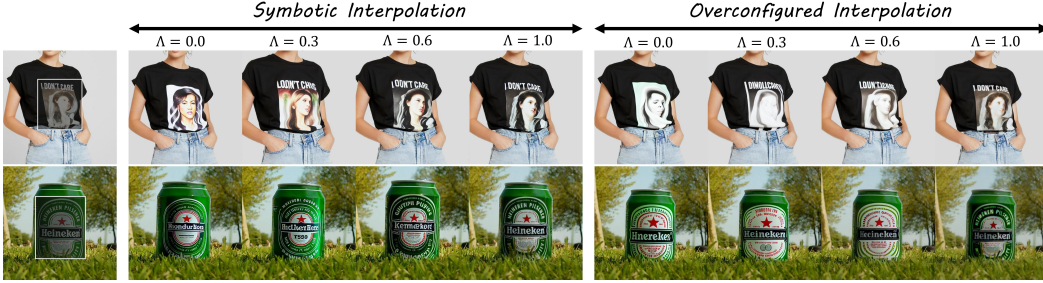


Figure 4: The comparison of the signature interpolation between the symbiotic system and overconfigured system, where the signature flows are delivered progressively with increasing threshold, ranging from the blocked states to the fully released states during inference. The symbiotic system manifests the consistent semantic content and comforting quality with flexible signature decoration.

Symbiotic Temperament. Peculiarly, the low-level signatures derived from the symbiotic diffusion system are highly semantic-independent, and the creative content generation capability is widely preserved even with the blocked signature flow $\epsilon_\theta(\mathbf{z}_t, t, \tau_\theta(\mathbf{c}), \emptyset)$, which is significantly different from the collapsed quality and diversity in overconfigured systems, as shown in Fig. 4. We suppose the auxiliary ζ_θ induces the leakage of the generative expertise from the entangled forward interdependence with denoising network ϵ_θ . Moreover, we show that the symbiotic system enjoys the continuous transmission space for progressive signature decoration with controllable signature flow.

3.3 Sparse Recycling

Albeit the scrupulous signature concentration, the overloaded transmission could cause the potential duplicate risk with ultimate subject fidelity and inferior scene conformity. Prior investigations settle the information bottleneck with suppressive transformation \mathcal{T} for signature delivering, including landmark representation and high-frequency map. However, the symbiotic diffusion system predefines the congruous status behavior, and requests the delivered subject within the same signal space as the denoising latents, *i.e.*, the identity \mathcal{T} , resulting in complete signature disclosure. In light of this, the sparse recycling paradigm is adopted for the symbiotic system with compressed transmission quota. Sidestep the transformation of the input signal, we randomly discard the self-delivered signatures within the denoising network at cached attention procedures in the content generation flow.

For consistency, we remain utilize \mathcal{T} to denote the suppressive transformation, and given by

$$\mathcal{T}_{\epsilon_i, \Lambda}(\mathbf{c}) = \begin{cases} \mathbf{z}_c^i, & \text{if } k \leq \Lambda \text{ and } k \sim \mathcal{U}(0, 1) \\ \emptyset, & \text{otherwise} \end{cases} \quad (5)$$

where k is sampled from the uniform distribution $\mathcal{U}(0, 1)$ for comparison with the threshold

Λ , \mathbf{z}_c^i is the cached subject signature at i -th attention procedure, \emptyset represents the null with discarding operation, $\mathcal{T}_{\epsilon_i, \Lambda}$ is the layer-wise transformation attached to the denoising network ϵ_θ that compress the signature flow. In particular, besides the prevention of the duplicated risk, the compressed transmission quota implicitly steers the diversified hyper-representations of the signature, facilitating the symbiotic system with improved subject transmission quality for scene harmonization, as shown in Tab. 1, which is also competent for the overconfigured system. Consequently, the denoising objective of the symbiotic diffusion system with sparse recycling is given by

$$\mathcal{L} = \mathbb{E}_{\mathbf{z}, \mathbf{c}, \epsilon, t} [\|\epsilon - \epsilon_\theta(\mathbf{z}_t, t, \tau_\theta(\mathbf{c}), \mathcal{T}_{\epsilon_\theta, \Lambda}(\mathbf{c}))\|_2^2], \quad (6)$$

where $\mathcal{T}_{\epsilon_\theta, \Lambda}$ is the collection of $\mathcal{T}_{\epsilon_i, \Lambda}$ along the denoising network. In inference, the sparse recycling is disabled in default with complete signature transmission, and enabled with continuous signature decoration. Additionally, the classifier-free guidance [72] is incorporated to provide the conditional direction, formulated as

$$\epsilon_{\theta, \mathbf{c}}(\mathbf{z}_t, t, w, \mathbf{c}) = \epsilon_\theta(\mathbf{z}_t, t, \emptyset, \emptyset) + w(\epsilon_\theta(\mathbf{z}_t, t, \tau_\theta(\mathbf{c}), \mathcal{T}_{\epsilon_\theta, \Lambda}(\mathbf{c})) - \epsilon_\theta(\mathbf{z}_t, t, \emptyset, \emptyset)), \quad (7)$$

where w is the guidance scale parameter.

Table 1: The transmission gain of the sparse recycling paradigm in delivering the faithful subject at both overconfigured system and symbiotic system.

Configured	CLIP-S \uparrow	LPIPS \downarrow	MUSIQ \uparrow
ControlNet	87.9 (+0.2)	0.141 (+0.004)	68.6 (+0.5)
ReferenceNet	90.2 (+0.4)	0.134 (+0.011)	68.2 (+0.6)
Recycling	91.3 (+0.3)	0.127 (+0.009)	68.9 (+0.8)



Figure 5: Qualitative comparison of AnyLogo and other competing methods on logo-level benchmark.

Table 2: Quantitative comparison with competing methods on logo-level benchmark. The subject fidelity are evaluated both from the semantic-level (CLIP-Score and DINO-Score) and signature-level (LPIPS), and the generated image quality is evaluated with MUSIQ.

Method	Logo				Virtual Tryon				Text Glyph			
	CLIP-S ↑	DINO-S ↑	LPIPS ↓	MUSIQ ↑	CLIP-S ↑	DINO-S ↑	LPIPS ↓	MUSIQ ↑	CLIP-S ↑	DINO-S ↑	LPIPS ↓	MUSIQ ↑
Paint-by-Example [17]	87.5	91.9	0.136	68.3	84.7	88.1	0.108	74.3	92.2	93.7	0.063	58.8
AnyDoor [35]	79.4	90.8	0.152	68.4	81.1	88.7	0.122	74.0	83.0	92.5	0.079	58.7
Graphit [77]	67.7	85.4	0.195	67.4	68.9	80.3	0.182	73.7	75.4	88.5	0.112	58.2
SD-Inpainting [1]	77.5	88.3	0.174	67.3	78.9	83.6	0.141	74.4	78.8	91.5	0.095	58.3
IP-Adapter [20]	82.7	89.9	0.148	68.0	82.1	84.9	0.125	73.9	83.4	91.2	0.083	58.7
AnyLogo (Ours)	91.3	92.5	0.127	68.9	91.4	94.0	0.082	74.6	95.0	96.5	0.049	58.8

3.4 Dataset Collection

As there is a lack of publicly available dataset that tailored for the logo-level customization with rich graphic patterns, we present the BrushLogo-70k, collecting from the open data source comprises wild logo detection dataset such as OpenLogo [73], OSLD [74], virtual tryon dataset with brand region such as Dresscode [75], VITON-HD [76], and text glyph dataset from AnyWord-3M [25]. The regions of interest are acquired with either ancillary provided or internal annotated, and the data are strictly excluded with irregular region size, aspect ratio, occlusion, and distortion quality. The detailed data composition is provided in the Appendix B. The evaluation set is constructed with 1k high-quality entities extracted from the collection with upraised criterions, referred as AnyLogo-Benchmark.

4 Experiments

4.1 Implementation Details

We implement AnyLogo based on the Stable Diffusion v1.5 for weights initialization, while the VAE module is replaced with the SDXL version for advanced regression quality. We train our model on constructed BrushLogo-70k dataset with 4 A800 GPUs for 50 000 steps. We preprocess the scene images with zoom-in strategy, and the subject images are augmented with horizontal flip, rotation, optical distortion, and super resolution. Image sizes are set to be 512×512. We choose AdamW optimizer with the fixed learning rate of 1×10^{-5} and the batch size of 64. The weighted sampling strategy is adopted for unbalanced data composition. The threshold in sparse recycling is set to be

Table 3: Comparison of the overconfigured system and the symbotic system on wild logo customization.

Methods	CLIP-S \uparrow	DINO-S \uparrow	LPIPS \downarrow	MUSIQ \uparrow	DIV \uparrow
Baseline	86.8	90.4	0.137	68.5	-
+ ControlNet	87.7	91.0	0.132	68.1	0.213
+ ReferenceNet	89.8	91.3	0.123	67.6	0.182
+ Model Recycling	91.0	92.1	0.118	68.1	0.279

Table 4: Ablation experiments of the recycling position in the denoising model for self-delivered signature transmission.

Position	CLIP-S \uparrow	DINO-S \uparrow	LPIPS \downarrow	MUSIQ \uparrow
Encoder	89.2	90.5	0.132	67.5
Decoder	91.0	92.1	0.118	68.1
Enc. + Dec.	90.3	91.7	0.127	67.7



Figure 6: Visual comparisons of the overconfigured systems with configured ControlNet and ReferenceNet, and the symbotic system with model recycling policy and sparse transmission quota.

0.6, and the conditional encoder is employed as DINOv2 [78] for visual semantic injection. During inference, we adopt the DDIM sampler with 20 denoising steps. More details in Appendix A.

Evaluation Metrics. The evaluation involves two aspects, the customized scenes region are supposed to be consistent with the provided subject, and the overall generated image should be photorealistic. To this end, we introduce the following four metrics, the CLIP-score and DINO-score are adopted for measuring the subject fidelity from the profile-level with the cosine similarity between the extracted embeddings of the customized region and the subject, and the LPIPS [79] is adopted for measuring the signature-level consistency. The quality assessment metric MUSIQ [80] is engaged to evaluate the authenticity and harmony of the overall generated image. Additionally, following [52], the diversified generation capability of the subject-driven diffusion system with blocked signature flow is further quantified with averaged LPIPS similarity between the generated images under the same subject.

Baselines. We perform the comparison with following zero-shot region customization methods, including Paint-by-Example [17], AnyDoor [35], Graphit [77], SD-Inpainting [1], and IP-Adapter [20]. SD-Inpainting is the text-driven method and we boost it with replaced CLIP image embeddings for subject transmission. IP-Adapter is implemented with inpainting version. The overconfigured system is implemented in the same experimental settings as AnyLogo for comparison, except for the extra configured ControlNet and ReferenceNet for signature delivering.

4.2 Comparison with Existing Alternatives

We provide the quantitative comparison results in Tab. 2, where the AnyLogo is superior in maintaining the signature consistency and semantic fidelity across diverse logo-level subjects, range from the wild brand logos, Tryon patterns, and text glyphs. It can be observed that the solitary semantic injection is stumbling for signature-preserved customization. Albeit the complementary hint signals strived by AnyDoor for signature transmission, the contour profile is informative insufficient with lossy compression, and more like spatial structure arrangement.

The qualitative results are presented in Fig. 5. Compared to the AnyLogo where the richly textured subjects are well transported to the candidate regions in the scene image with less distortion, other alternatives struggle in delivering the accurate low-level signatures with coarse semantic consistency, deviating from the color, pattern structure, and hallucination rendering. It would be conscious that the signature-level consistency is dramatically differ from the object-level concentration, where the dispersed and disconnected subjects are toilsome to be grasped against the strongly semantic compact entity, and the interleaved text and graphic layout form the raised challenge.



Figure 8: Outpainting results of AnyLogo, where the subject regions are preserved with absolute accuracy, and the scene background are regenerated with diversified presentation. The users are free to shift and scale the subject area for arbitrary highlighting display.

4.3 Ablation Study

Overconfigured System. We provide the comparison against the overconfigured system in Tab. 3 with extra equipped ControlNet and ReferenceNet. The baseline denotes the blocked signature flow with purely semantic injection. It can be observed that albeit the improved faithfulness with extra configured signature extractor, the model recycling policy with self-delivered signatures achieves the excellent fidelity. Note that the sparse recycling is excluded for validation. The visual comparisons are provided in Fig. 6, where the transmission distortion of the overconfigured system are manifested as distorted color and structure compared to the symbiotic system. We further evaluate the diversity of the two systems with disabled signature flow, where the symbiotic system exhibit the higher diversity as quantified in Tab. 3, owing to the holistic system construction that preclude the entangled generative expertise leakage, and the visual comparisons are shown in Fig. 4.

Position of the transmission. In Tab. 4, we provide the ablation experiments about the transmission position of the signature flow in model recycling policy. It can be observed that the transmission is efficient in the decoder part and encounters the obstacle in the encoder, which imply that the shallow layers are not well prepared with the steady semantic layout for signature delivering, and the overloaded signatures are undesirable during the content infancy.

Sparse Threshold λ . The sparse recycling paradigm is evaluated in Fig. 7 with various transmission thresholds in optimization and fully released in inference. We present the comparison curves both from the subject fidelity and image quality. The uncompressed signature transmission induces the harmed image quality with disharmonious duplicated risk, also shown in Fig. 6. The blocked signature flow manifests the restricted subject consistency with purely semantic injection. Combined with sparse recycling, the symbiotic system is much more efficient on semantic-relevant signature concentration with excluded signature noise.

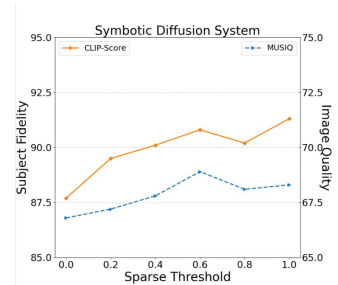


Figure 7: Tendency of sparse recycling with progressive signature delivering thresholds.

4.4 Discussion about the Fidelity and Future Works

We show that AnyLogo is not only proficient in region customization with arbitrary user provided subjects, but also favour the diversified outpainting with faithful subject highlight, as shown in Fig. 8, where the subject regions are preserved with absolute accuracy, and the scene background are regenerated with diversified presentation. We are delighting to point that these are two ways to maintain the signature-level consistency. In case of the lower fidelity requests for the scene region, it is of great potential to preserve the subject area for definitive fidelity with scale and shift manipulation, and the desired background could be complemented with semantic-faithful practices. We note that the outpainting version of AnyLogo is effortless to be implemented with simply reversing the binary mask of the scene image both in input space and latents complementary.

5 Conclusion

In this work, we proposed AnyLogo, a symbiotic subject-driven diffusion system with remarkable low-level signature consistency. Streamlined as vanilla image generation, we discern that the imperative customized gemini status, *i.e.*, the rigorous signature extraction and creative content generation can be systematically recycled within a single denoising model and are promisingly compatible. The model recycling policy promotes the reinforced subject transmission efficiency with alleviated systematic coherence, and the disentangled semantic-signature space with continuous signature decoration. Besides, the sparse recycling paradigm is adopted to prevent the potential duplicated risk with compressed transmission quota for diversified signature stimulation. Extensive experiments on constructed AnyLogo-Benchmark demonstrate the effectiveness and practicability of our method.

References

- [1] Robin Rombach, Andreas Blattmann, Dominik Lorenz, Patrick Esser, and Björn Ommer. High-resolution image synthesis with latent diffusion models. In *Proceedings of the IEEE/CVF conference on computer vision and pattern recognition*, pages 10684–10695, 2022.
- [2] Dustin Podell, Zion English, Kyle Lacey, Andreas Blattmann, Tim Dockhorn, Jonas Müller, Joe Penna, and Robin Rombach. Sdxl: Improving latent diffusion models for high-resolution image synthesis. In *The Twelfth International Conference on Learning Representations*, 2023.
- [3] Aditya Ramesh, Prafulla Dhariwal, Alex Nichol, Casey Chu, and Mark Chen. Hierarchical text-conditional image generation with clip latents. *arXiv preprint arXiv:2204.06125*, 1(2):3, 2022.
- [4] Chitwan Saharia, William Chan, Saurabh Saxena, Lala Li, Jay Whang, Emily L Denton, Kamyar Ghasemipour, Raphael Gontijo Lopes, Burcu Karagol Ayan, Tim Salimans, et al. Photorealistic text-to-image diffusion models with deep language understanding. *Advances in neural information processing systems*, 35:36479–36494, 2022.
- [5] Tim Brooks, Aleksander Holynski, and Alexei A Efros. Instructpix2pix: Learning to follow image editing instructions. In *Proceedings of the IEEE/CVF Conference on Computer Vision and Pattern Recognition*, pages 18392–18402, 2023.
- [6] Bahjat Kawar, Shiran Zada, Oran Lang, Omer Tov, Huiwen Chang, Tali Dekel, Inbar Mosseri, and Michal Irani. Imagic: Text-based real image editing with diffusion models. In *Proceedings of the IEEE/CVF Conference on Computer Vision and Pattern Recognition*, pages 6007–6017, 2023.
- [7] Amir Hertz, Ron Mokady, Jay Tenenbaum, Kfir Aberman, Yael Pritch, and Daniel Cohen-or. Prompt-to-prompt image editing with cross-attention control. In *The Eleventh International Conference on Learning Representations*, 2022.
- [8] Hexiang Hu, Kelvin CK Chan, Yu-Chuan Su, Wenhui Chen, Yandong Li, Kihyuk Sohn, Yang Zhao, Xue Ben, Boqing Gong, William Cohen, et al. Instruct-imagen: Image generation with multi-modal instruction. *arXiv preprint arXiv:2401.01952*, 2024.
- [9] Tim Brooks, Bill Peebles, Connor Holmes, Will DePue, Yufei Guo, Li Jing, David Schnurr, Joe Taylor, Troy Luhman, Eric Luhman, Clarence Ng, Ricky Wang, and Aditya Ramesh. Video generation models as world simulators. 2024.
- [10] Omer Bar-Tal, Hila Chefer, Omer Tov, Charles Herrmann, Roni Paiss, Shiran Zada, Ariel Ephrat, Junhwa Hur, Yuanzhen Li, Tomer Michaeli, et al. Lumiere: A space-time diffusion model for video generation. *arXiv preprint arXiv:2401.12945*, 2024.
- [11] Patrick Esser, Johnathan Chiu, Parmida Atighehchian, Jonathan Granskog, and Anastasis Germanidis. Structure and content-guided video synthesis with diffusion models. In *Proceedings of the IEEE/CVF International Conference on Computer Vision*, pages 7346–7356, 2023.
- [12] Fuchen Long, Zhaofan Qiu, Ting Yao, and Tao Mei. Videodrafter: Content-consistent multi-scene video generation with llm. *arXiv preprint arXiv:2401.01256*, 2024.
- [13] Lin Zhang, Shentong Mo, Yijing Zhang, and Pedro Morgado. Audio-synchronized visual animation. *arXiv preprint arXiv:2403.05659*, 2024.

- [14] Xu He, Qiaochu Huang, Zhensong Zhang, Zhiwei Lin, Zhiyong Wu, Sicheng Yang, Minglei Li, Zhiyi Chen, Songcen Xu, and Xiaofei Wu. Co-speech gesture video generation via motion-decoupled diffusion model. *arXiv preprint arXiv:2404.01862*, 2024.
- [15] Zachary Novack, Julian McAuley, Taylor Berg-Kirkpatrick, and Nicholas J Bryan. Ditto: Diffusion inference-time t-optimization for music generation. *arXiv preprint arXiv:2401.12179*, 2024.
- [16] Shuai Tan, Bin Ji, Mengxiao Bi, and Ye Pan. Edtalk: Efficient disentanglement for emotional talking head synthesis. *arXiv preprint arXiv:2404.01647*, 2024.
- [17] Binxin Yang, Shuyang Gu, Bo Zhang, Ting Zhang, Xuejin Chen, Xiaoyan Sun, Dong Chen, and Fang Wen. Paint by example: Exemplar-based image editing with diffusion models. In *Proceedings of the IEEE/CVF Conference on Computer Vision and Pattern Recognition*, pages 18381–18391, 2023.
- [18] Yizhi Song, Zhifei Zhang, Zhe Lin, Scott Cohen, Brian Price, Jianming Zhang, Soo Ye Kim, and Daniel Aliaga. Objectstitch: Object compositing with diffusion model. In *Proceedings of the IEEE/CVF Conference on Computer Vision and Pattern Recognition*, pages 18310–18319, 2023.
- [19] Yulin Pan, Chaojie Mao, Zeyinzi Jiang, Zhen Han, and Jingfeng Zhang. Locate, assign, refine: Taming customized image inpainting with text-subject guidance. *arXiv preprint arXiv:2403.19534*, 2024.
- [20] Hu Ye, Jun Zhang, Sibao Liu, Xiao Han, and Wei Yang. Ip-adapter: Text compatible image prompt adapter for text-to-image diffusion models. *arXiv preprint arXiv:2308.06721*, 2023.
- [21] Zhen Li, Mingdeng Cao, Xintao Wang, Zhongang Qi, Ming-Ming Cheng, and Ying Shan. Photomaker: Customizing realistic human photos via stacked id embedding. *arXiv preprint arXiv:2312.04461*, 2023.
- [22] Qinghe Wang, Xu Jia, Xiaomin Li, Taiqing Li, Liqian Ma, Yunzhi Zhuge, and Huchuan Lu. Stableidentity: Inserting anybody into anywhere at first sight. *arXiv preprint arXiv:2401.15975*, 2024.
- [23] Yuxuan Yan, Chi Zhang, Rui Wang, Yichao Zhou, Gege Zhang, Pei Cheng, Gang Yu, and Bin Fu. Facestudio: Put your face everywhere in seconds. *arXiv preprint arXiv:2312.02663*, 2023.
- [24] Zhuowei Chen, Shancheng Fang, Wei Liu, Qian He, Mengqi Huang, Yongdong Zhang, and Zhendong Mao. Dreamidentity: Improved editability for efficient face-identity preserved image generation. *arXiv preprint arXiv:2307.00300*, 2023.
- [25] Yuxiang Tuo, Wangmeng Xiang, Jun-Yan He, Yifeng Geng, and Xuansong Xie. Anytext: Multilingual visual text generation and editing. In *The Twelfth International Conference on Learning Representations*, 2023.
- [26] Jingye Chen, Yupan Huang, Tengchao Lv, Lei Cui, Qifeng Chen, and Furu Wei. Textdiffuser: Diffusion models as text painters. *Advances in Neural Information Processing Systems*, 36, 2023.
- [27] Lingjun Zhang, Xinyuan Chen, Yaohui Wang, Yue Lu, and Yu Qiao. Brush your text: Synthesize any scene text on images via diffusion model. In *Proceedings of the AAAI Conference on Artificial Intelligence*, volume 38, pages 7215–7223, 2024.
- [28] Tan Wang, Linjie Li, Kevin Lin, Chung-Ching Lin, Zhengyuan Yang, Hanwang Zhang, Zicheng Liu, and Lijuan Wang. Disco: Disentangled control for referring human dance generation in real world. *arXiv e-prints*, pages arXiv–2307, 2023.
- [29] Li Hu, Xin Gao, Peng Zhang, Ke Sun, Bang Zhang, and Liefeng Bo. Animate anyone: Consistent and controllable image-to-video synthesis for character animation. *arXiv preprint arXiv:2311.17117*, 2023.
- [30] Zhongcong Xu, Jianfeng Zhang, Jun Hao Liew, Hanshu Yan, Jia-Wei Liu, Chenxu Zhang, Jiashi Feng, and Mike Zheng Shou. Magicanimate: Temporally consistent human image animation using diffusion model. *arXiv preprint arXiv:2311.16498*, 2023.
- [31] Yue Ma, Yingqing He, Hongfa Wang, Andong Wang, Chenyang Qi, Chengfei Cai, Xiu Li, Zhifeng Li, Heung-Yeung Shum, Wei Liu, et al. Follow-your-click: Open-domain regional image animation via short prompts. *arXiv preprint arXiv:2403.08268*, 2024.

- [32] Mehmet Saygin Seyfioglu, Karim Bouyarmane, Suren Kumar, Amir Tavanaei, and Ismail B Tutar. Diffuse to choose: Enriching image conditioned inpainting in latent diffusion models for virtual try-all. *arXiv preprint arXiv:2401.13795*, 2024.
- [33] Yanlong Zang, Han Yang, Jiaxu Miao, and Yi Yang. Product-level try-on: Characteristics-preserving try-on with realistic clothes shading and wrinkles. *arXiv preprint arXiv:2401.11239*, 2024.
- [34] Jeffrey Zhang, Kedan Li, Shao-Yu Chang, and David Forsyth. Acdg-vton: Accurate and contained diffusion generation for virtual try-on. *arXiv preprint arXiv:2403.13951*, 2024.
- [35] Xi Chen, Lianghua Huang, Yu Liu, Yujun Shen, Deli Zhao, and Hengshuang Zhao. Anydoor: Zero-shot object-level image customization. *arXiv preprint arXiv:2307.09481*, 2023.
- [36] Qixun Wang, Xu Bai, Haofan Wang, Zekui Qin, and Anthony Chen. Instantid: Zero-shot identity-preserving generation in seconds. *arXiv preprint arXiv:2401.07519*, 2024.
- [37] Alex Nichol, Prafulla Dhariwal, Aditya Ramesh, Pranav Shyam, Pamela Mishkin, Bob McGrew, Ilya Sutskever, and Mark Chen. Glide: Towards photorealistic image generation and editing with text-guided diffusion models. *arXiv preprint arXiv:2112.10741*, 2021.
- [38] Omri Avrahami, Dani Lischinski, and Ohad Fried. Blended diffusion for text-driven editing of natural images. In *Proceedings of the IEEE/CVF Conference on Computer Vision and Pattern Recognition*, pages 18208–18218, 2022.
- [39] Junhao Zhuang, Yanhong Zeng, Wenran Liu, Chun Yuan, and Kai Chen. A task is worth one word: Learning with task prompts for high-quality versatile image inpainting. *arXiv preprint arXiv:2312.03594*, 2023.
- [40] Hayk Manukyan, Andranik Sargsyan, Barsegh Atanyan, Zhangyang Wang, Shant Navasardyan, and Humphrey Shi. Hd-painter: High-resolution and prompt-faithful text-guided image inpainting with diffusion models. *arXiv preprint arXiv:2312.14091*, 2023.
- [41] Ben Xue, Shenghui Ran, Quan Chen, Rongfei Jia, Binqiang Zhao, and Xing Tang. Dccf: Deep comprehensible color filter learning framework for high-resolution image harmonization. In *European Conference on Computer Vision*, pages 300–316. Springer, 2022.
- [42] Haoxing Chen, Zhangxuan Gu, Yaohui Li, Jun Lan, Changhua Meng, Weiqiang Wang, and Huaxiong Li. Hierarchical dynamic image harmonization. In *Proceedings of the 31st ACM International Conference on Multimedia*, pages 1422–1430, 2023.
- [43] Lingzhi Zhang, Tarmily Wen, and Jianbo Shi. Deep image blending. In *Proceedings of the IEEE/CVF winter conference on applications of computer vision*, pages 231–240, 2020.
- [44] Huikai Wu, Shuai Zheng, Junge Zhang, and Kaiqi Huang. Gp-gan: Towards realistic high-resolution image blending. In *Proceedings of the 27th ACM international conference on multimedia*, pages 2487–2495, 2019.
- [45] Samaneh Azadi, Deepak Pathak, Sayna Ebrahimi, and Trevor Darrell. Compositional gan: Learning image-conditional binary composition. *International Journal of Computer Vision*, 128(10):2570–2585, 2020.
- [46] Chen-Hsuan Lin, Ersin Yumer, Oliver Wang, Eli Shechtman, and Simon Lucey. St-gan: Spatial transformer generative adversarial networks for image compositing. In *Proceedings of the IEEE conference on computer vision and pattern recognition*, pages 9455–9464, 2018.
- [47] Tao Yu, Runseng Feng, Ruoyu Feng, Jinming Liu, Xin Jin, Wenjun Zeng, and Zhibo Chen. Inpaint anything: Segment anything meets image inpainting. *arXiv preprint arXiv:2304.06790*, 2023.
- [48] Shilin Lu, Yanzhu Liu, and Adams Wai-Kin Kong. Tf-icon: Diffusion-based training-free cross-domain image composition. In *Proceedings of the IEEE/CVF International Conference on Computer Vision*, pages 2294–2305, 2023.
- [49] Yibin Wang, Weizhong Zhang, Jianwei Zheng, and Cheng Jin. Primecomposer: Faster progressively combined diffusion for image composition with attention steering. *arXiv preprint arXiv:2403.05053*, 2024.
- [50] Xin Zhang, Jiaxian Guo, Paul Yoo, Yutaka Matsuo, and Yusuke Iwasawa. Paste, inpaint and harmonize via denoising: Subject-driven image editing with pre-trained diffusion model. *arXiv preprint arXiv:2306.07596*, 2023.

- [51] Wei Li, Xue Xu, Jiachen Liu, and Xinyan Xiao. Unimo-g: Unified image generation through multimodal conditional diffusion. *arXiv preprint arXiv:2401.13388*, 2024.
- [52] Nataniel Ruiz, Yuanzhen Li, Varun Jampani, Yael Pritch, Michael Rubinstein, and Kfir Aberman. Dreambooth: Fine tuning text-to-image diffusion models for subject-driven generation. In *Proceedings of the IEEE/CVF Conference on Computer Vision and Pattern Recognition*, pages 22500–22510, 2023.
- [53] Rinon Gal, Yuval Alaluf, Yuval Atzmon, Or Patashnik, Amit H Bermano, Gal Chechik, and Daniel Cohen-Or. An image is worth one word: Personalizing text-to-image generation using textual inversion. *arXiv preprint arXiv:2208.01618*, 2022.
- [54] Yuchao Gu, Xintao Wang, Jay Zhangjie Wu, Yujun Shi, Yunpeng Chen, Zihan Fan, Wuyou Xiao, Rui Zhao, Shuning Chang, Weijia Wu, et al. Mix-of-show: Decentralized low-rank adaptation for multi-concept customization of diffusion models. *Advances in Neural Information Processing Systems*, 36, 2023.
- [55] Nupur Kumari, Bingliang Zhang, Richard Zhang, Eli Shechtman, and Jun-Yan Zhu. Multi-concept customization of text-to-image diffusion. In *Proceedings of the IEEE/CVF Conference on Computer Vision and Pattern Recognition*, pages 1931–1941, 2023.
- [56] Zhiheng Liu, Yifei Zhang, Yujun Shen, Kecheng Zheng, Kai Zhu, Ruili Feng, Yu Liu, Deli Zhao, Jingren Zhou, and Yang Cao. Cones 2: Customizable image synthesis with multiple subjects. *arXiv preprint arXiv:2305.19327*, 2023.
- [57] Mengyang Feng, Jinlin Liu, Kai Yu, Yuan Yao, Zheng Hui, Xiefan Guo, Xianhui Lin, Haolan Xue, Chen Shi, Xiaowen Li, et al. Dreamoving: A human video generation framework based on diffusion models. *arXiv e-prints*, pages arXiv–2312, 2023.
- [58] Mingdeng Cao, Xintao Wang, Zhongang Qi, Ying Shan, Xiaohu Qie, and Yinqiang Zheng. Masactrl: Tuning-free mutual self-attention control for consistent image synthesis and editing. In *Proceedings of the IEEE/CVF International Conference on Computer Vision*, pages 22560–22570, 2023.
- [59] Sihan Xu, Yidong Huang, Jiayi Pan, Ziqiao Ma, and Joyce Chai. Inversion-free image editing with natural language. *arXiv preprint arXiv:2312.04965*, 2023.
- [60] Jascha Sohl-Dickstein, Eric Weiss, Niru Maheswaranathan, and Surya Ganguli. Deep unsupervised learning using nonequilibrium thermodynamics. In *International conference on machine learning*, pages 2256–2265. PMLR, 2015.
- [61] Jonathan Ho, Ajay Jain, and Pieter Abbeel. Denoising diffusion probabilistic models. *Advances in neural information processing systems*, 33:6840–6851, 2020.
- [62] Yang Song and Stefano Ermon. Generative modeling by estimating gradients of the data distribution. *Advances in neural information processing systems*, 32, 2019.
- [63] Yang Song, Jascha Sohl-Dickstein, Diederik P Kingma, Abhishek Kumar, Stefano Ermon, and Ben Poole. Score-based generative modeling through stochastic differential equations. In *International Conference on Learning Representations*, 2020.
- [64] Kevin Clark and Priyank Jaini. Text-to-image diffusion models are zero shot classifiers. *Advances in Neural Information Processing Systems*, 36, 2023.
- [65] Quang Nguyen, Truong Vu, Anh Tran, and Khoi Nguyen. Dataset diffusion: Diffusion-based synthetic data generation for pixel-level semantic segmentation. *Advances in Neural Information Processing Systems*, 36, 2023.
- [66] Mengyu Wang, Henghui Ding, Jun Hao Liew, Jiajun Liu, Yao Zhao, and Yunchao Wei. Seg-refiner: Towards model-agnostic segmentation refinement with discrete diffusion process. In *Thirty-seventh Conference on Neural Information Processing Systems*, 2023.
- [67] Narek Tumanyan, Michal Geyer, Shai Bagon, and Tali Dekel. Plug-and-play diffusion features for text-driven image-to-image translation. In *Proceedings of the IEEE/CVF Conference on Computer Vision and Pattern Recognition*, pages 1921–1930, 2023.
- [68] Bingyan Liu, Chengyu Wang, Tingfeng Cao, Kui Jia, and Jun Huang. Towards understanding cross and self-attention in stable diffusion for text-guided image editing. *arXiv preprint arXiv:2403.03431*, 2024.

- [69] Animesh Karnewar, Andrea Vedaldi, David Novotny, and Niloy J Mitra. Holodiffusion: Training a 3d diffusion model using 2d images. In *Proceedings of the IEEE/CVF conference on computer vision and pattern recognition*, pages 18423–18433, 2023.
- [70] Junshu Tang, Tengfei Wang, Bo Zhang, Ting Zhang, Ran Yi, Lizhuang Ma, and Dong Chen. Make-it-3d: High-fidelity 3d creation from a single image with diffusion prior. In *Proceedings of the IEEE/CVF International Conference on Computer Vision*, pages 22819–22829, 2023.
- [71] Seongmin Hong, Kyeonghyun Lee, Suh Yoon Jeon, Hyewon Bae, and Se Young Chun. On exact inversion of dpm-solvers, 2023.
- [72] Jonathan Ho and Tim Salimans. Classifier-free diffusion guidance. In *NeurIPS 2021 Workshop on Deep Generative Models and Downstream Applications*, 2021.
- [73] Hang Su, Xiatian Zhu, and Shaogang Gong. Open logo detection challenge. In *British Machine Vision Conference*, 2018.
- [74] Muhammet Bastan, Hao-Yu Wu, Tian Cao, Bhargava Kota, and Mehmet Tek. Large scale open-set deep logo detection. *arXiv preprint arXiv:1911.07440*, 2019.
- [75] Davide Morelli, Matteo Fincato, Marcella Cornia, Federico Landi, Fabio Cesari, and Rita Cucchiara. Dress Code: High-Resolution Multi-Category Virtual Try-On. In *Proceedings of the European Conference on Computer Vision*, 2022.
- [76] Seunghwan Choi, Sunghyun Park, Minsoo Lee, and Jaegul Choo. Viton-hd: High-resolution virtual try-on via misalignment-aware normalization. In *Proc. of the IEEE conference on computer vision and pattern recognition (CVPR)*, 2021.
- [77] <https://github.com/navervision/Graphit>. Graphit: A unified framework for diverse image editing tasks. In *Github Project*, 2023.
- [78] Maxime Oquab, Timothée Darcet, Théo Moutakanni, Huy Vo, Marc Szafraniec, Vasil Khalidov, Pierre Fernandez, Daniel Haziza, Francisco Massa, Alaaeldin El-Nouby, et al. Dinov2: Learning robust visual features without supervision. *arXiv preprint arXiv:2304.07193*, 2023.
- [79] Richard Zhang, Phillip Isola, Alexei A Efros, Eli Shechtman, and Oliver Wang. The unreasonable effectiveness of deep features as a perceptual metric. In *Proceedings of the IEEE conference on computer vision and pattern recognition*, pages 586–595, 2018.
- [80] Junjie Ke, Qifei Wang, Yilin Wang, Peyman Milanfar, and Feng Yang. Musiq: Multi-scale image quality transformer. In *Proceedings of the IEEE/CVF international conference on computer vision*, pages 5148–5157, 2021.
- [81] Jianyi Wang, Kelvin CK Chan, and Chen Change Loy. Exploring clip for assessing the look and feel of images. In *Proceedings of the AAAI Conference on Artificial Intelligence*, volume 37, pages 2555–2563, 2023.
- [82] Pierre Fernandez, Guillaume Couairon, Hervé Jégou, Matthijs Douze, and Teddy Furon. The stable signature: Rooting watermarks in latent diffusion models. In *Proceedings of the IEEE/CVF International Conference on Computer Vision*, pages 22466–22477, 2023.
- [83] Senthil Purushwalkam, Akash Gokul, Shafiq Joty, and Nikhil Naik. Bootpig: Bootstrapping zero-shot personalized image generation capabilities in pretrained diffusion models. *arXiv preprint arXiv:2401.13974*, 2024.

A More Model Details

We implement the conditional encoder τ_θ with hierarchical DINOv2 features for semantic injection, which conducted at all cross attention layers of the denoising model. Specifically, we extract four group of embeddings from the DINOv2 that corresponding to the four scales of the denoising model. And each embedding incorporates the spatial patch tokens with size of $\mathbb{R}^{257 \times 1024}$ and broadly dsitributed from the shallow to deeper layers with step size of 6. The extracted four group of semantic embeddings are progressively injected to the denoising model with symmetrical variation between encoder and decoder. To perceive the background of the scene image for harmony subject transmission, we incorporates the additional background embedding that concatenates to the each group of subject embedding, which extracted in the same hierarchical manner, and each background embedding is only represented by single global token in size of $\mathbb{R}^{1 \times 1024}$ to exclude the scene details.

B Data Compositions

The detailed data composition of the BrushLogo-70k and AnyLogo-Benchmark is illustrated in Tab 5, which are adopted as train set and test set, respectively. As presented in sec 3.4, the wild logo are collected from the OpenLogo [73] and OSLD [74] with 23,947 and 25,955 subject-scene pairs, the brands in virtual tryon are collectd from the Dresscode [75] and VITON-HD [76] with 5,434 and 2,986 pairs, and the text glyph are collected from the AnyWord-3M-Laion [25] with 13,778 pairs. The test set is constructed with 1k high-quality pairs extracted from the aforementioned collections with upraised criterions. The data are filtered with CLIP-IQA [81] from three dimensions with prompts of quality, contrast, and sharpness. Apart from that, the irregular region size and aspect ratio are excluded. The regions of the logo pattern or text in the scene images are acquired with either ancillary provided (wild logo and text glyph) or internal annotated (virtual tryon). The subjects are paired with high DINO-similarity from other entities under the same brand for the wild logo, and provided with paired product in the virtual tryon. The subjects for text are extracted from its own scene images to prevent glyph distortion.

Table 5: The composition of the collected dataset.

Data Split	Wild Logo	Virtual Tryon	Text Glyph
BrushLogo-70k	49382	8420	13492
AnyLogo-Benchmark	520	223	286

C Limitations

The limitations are encountered with two main problems, as shown in Fig. 9. The first is the unmatched aspect ratio between the subject and the customized region in scene image. In order to maintain the subject fidelity with less distortion, we do not perform the resize operation in preprocessing, and the transmission are tend to repeat the subject with original ratio to fill the specified region. The second is the hallucination that related to the scene image, which is also occurred with unmatched aspect ratio between the subject and the customized region. And the model tends to hallucinate the new concept that related to the background of the scene image, *e.g.*, the side windows for the car, to fill the candidate region.



Figure 9: The failure cases. The model tends to repeat the subject or hallucinate the new concept to fill the customized region when encounters the unmatched aspect ratio.

D Boarder Impacts

The ability to manipulate logos could be benefit for product promotion, poster making, logo alteration in advertising position, *etc.*, and the outpaiting version with diversified highlighting backgrounds could ease the cost of the venue rental and model hiring. However, the misuse could incur the potential copyright problems with legal disputes. And the generative logos may confuse the consumers to discern the authenticity and impact the reputation of the brands. Furthermore, the population of the

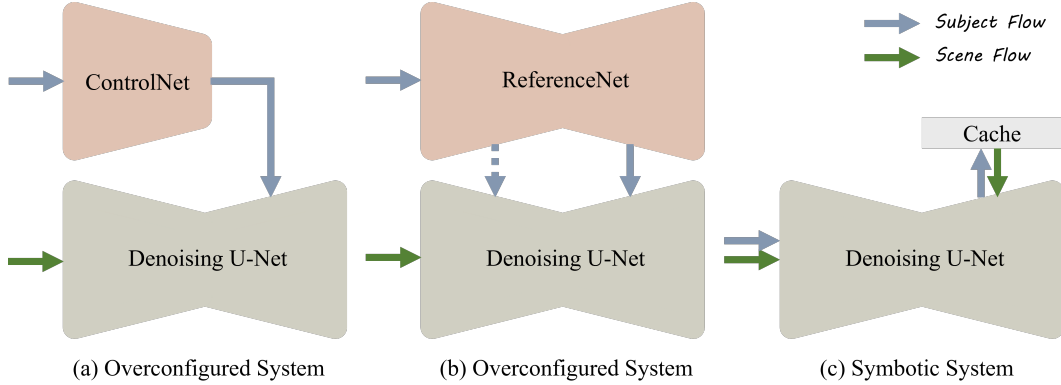


Figure 10: An illustration of the overconfigured diffusion system with extra configured ControlNet and ReferenceNet, and the symbiotic diffusion system with model recycling, for subject customization.

generative models could impact the graphic designers and brand professionals, as the automated logo alteration with similar semantic layout might reduce the demand for manual design work. We preclude the copyright infringement with infused watermarks [82] to fingerprint the generated images.

E Comparison of the Overconfigured System and Symbiotic System

We provide the detailed illustration of the overconfigured diffusion system and the symbiotic diffusion system for subject customization in Fig. 10. As can be seen that the overconfigured system employ the individual model to extract the signatures of the subject for reinforced detail enhancement, with progressive residual complement in ControlNet [25, 27, 33, 35, 32], and hierarchical spatial attention in ReferenceNet [29, 30, 36, 83]. The symbiotic diffusion system is built upon the model recycling policy with eliminated signature-relevant model configurations, and the signature extraction and content generation are systematically recycled within a single denoising model.

We provide the detailed calculation process of the Fig. 1, where the transmitted statistic latent difference (SLD) is calculated with ℓ_1 error of the average between the delivered subject latents and corresponding denoising latents in the delivered layer. We provide four layers comparison along the denoising model, including the middle-attention0, up1-attention2, up2-attention2, and up3-attention2, where the middle refers to the middle block of the denoising model, up refers to the decoder of the denoising model, and attention refers to the self-attention layer. It can be observed that the overconfigured system exhibits the larger statistic discrepancy between the delivered subject latents and corresponding denoising latents, compared to the symbiotic system, owing to the external engagement that breaks the statistic coherence. Consequently, the accumulative subject attention (ASA) is significantly hampered, as shown in the shadow region of the Fig 1 (a), which calculated with proportion of the accumulated attention score of the subject against the overall attention map in the delivered self-attention layers

F More Visual Comparisons

We provide the visual results of AnyLogo on object-level customization in Fig. 11, without tuning. It can be observed that AnyLogo is proficient in rendering the portrait of the natural object for personali-



Figure 11: Visual results of AnyLogo on object customization.

Subject	Scene	PBE	AnyDoor	+ ControlNet	+ ReferenceNet	AnyLogo
OUTREACH	ELVIS COSTELLO UNFAITHFUL MUSIC SOUNDTRACK ALBUM	OUTREACH COSTELLO UNFAITHFUL MUSIC SOUNDTRACK ALBUM	SUDNACH COSTELLO UNFAITHFUL MUSIC SOUNDTRACK ALBUM	OUTREACT COSTELLO UNFAITHFUL MUSIC SOUNDTRACK ALBUM	OUTREACH COSTELLO UNFAITHFUL MUSIC SOUNDTRACK ALBUM	OUTREACH COSTELLO UNFAITHFUL MUSIC SOUNDTRACK ALBUM
	RIVIERA GOLDEN ALBUM GOLDEN BOMBER	GOLDEN RVIZRR GOLDEN BOMBER	GOLDEN MOIBB? GOLDEN BOMBER	GOLDEN RIVERA GOLDEN BOMBER	GOLDEN RIVIERA GOLDEN BOMBER	GOLDEN RIVIERA GOLDEN BOMBER
Lee						
FIORUCCI						
NBC						
Dr. Comfort						
TESLA						

Figure 12: Visual comparison of AnyLogo and other competing methods on logo-level benchmark.

zation, which is applicable to customize the user assets with personalized preference, such as pet and favoured cuisine.

In Fig. 12, we provide more visual comparison results of AnyLogo with other competing methods on logo-level customization, together with the overconfigured system equipped by ControlNet and ReferenceNet for visual ablation. It can be observed that AnyLogo is proficient in maintaining the subject-specific signatures rather than hallucinating the general semantics, including curve contour, graphic layout, *etc.*, and dealing well with the scene background, such as occlusion.